Eur. Phys. J. D **46**, 545–560 (2008)
DOI: 10.1140/epjd/e2008-00016-4

THE EUROPEAN PHYSICAL JOURNAL D

Ultracold atoms in optical lattices generated by quantized light fields

C. Maschler[1,a], I.B. Mekhov[1,2], and H. Ritsch[1]

[1] Institut für theoretische Physik, Universität Innsbruck, Technikerstr. 25, 6020 Innsbruck, Austria
[2] St. Petersburg State University, Faculty of Physics, St. Petersburg, Russia

Received 23 October 2007 / Received in final form 22 December 2007
Published online 6 February 2008 –

Abstract. We study an ultracold gas of neutral atoms subject to the periodic optical potential generated by a high-Q cavity mode. In the limit of very low temperatures, cavity field and atomic dynamics require a quantum description. Starting from a cavity QED single atom Hamiltonian we use different routes to derive approximative multiparticle Hamiltonians in Bose-Hubbard form with rescaled or even dynamical parameters. In the limit of large enough cavity damping the different models agree. Compared to free space optical lattices, quantum uncertainties of the potential and the possibility of atom-field entanglement lead to modified phase transition characteristics, the appearance of new phases or even quantum superpositions of different phases. Using a corresponding effective master equation, which can be numerically solved for few particles, we can study time evolution including dissipation. As an example we exhibit the microscopic processes behind the transition dynamics from a Mott insulator like state to a self-ordered superradiant state of the atoms, which appears as steady state for transverse atomic pumping.

PACS. 42.50.Pq Cavity quantum electrodynamics; micromasers – 37.10.Jk Atoms in optical lattices – 03.75.Lm Tunneling, Josephson effect, Bose-Einstein condensates in periodic potentials, solitons, vortices, and topological excitations

Highlight Paper

1 Introduction

Laser light, far red detuned from an atomic resonance, is nowadays a standard tool in experimental quantum optics to create tunable optical potentials [1] which can be loaded with ultracold atoms to provide for a plethora of possibilities to study quantum properties of many-body strongly correlated systems [2]. The high level of microscopic understanding and extensive control of the light fields and atoms allow to implement genuine models like e.g. the Bose-Hubbard (BH) model [3,4]. Initially originating from condensed matter physics [5] it has been used to study the Mott insulator to superfluid phase transition [6] in detail and in real time. Adjusting several of the lattice parameters as the intensity and the configuration of the lattice lasers provides a versatile toolbox of techniques to control the dynamics of the atoms in the lattice [7]. Moreover, the collisional properties of the certain types of atoms can be tailored by means of magnetic [8] or optical [9] Feshbach resonances. Using extra confinement it was even possible to observe the Mott insulator to superfluid transition in 1D [10,11] and 2D [12], followed by other spectacular demonstrations of condensed matter physics phenomena as the realization of a Tonks gas in 1D [13,14] and the Berezinskii-Kosterlitz-Thouless phase transition in 2D [15]. Theoretically many more proposals to apply these methods to spin systems and investigate further fascinating properties of strongly correlated systems were put forward (see [16] for a review).

In all of these approaches, the light fields were approximated by classical, externally prescribed fields independent of the atoms. This requires intense light, far detuned from any atomic transition. Of course this assumption holds no longer if the light, which generates the optical lattice, is enhanced by an optical resonator. In this case — given a sufficient atom number N and atom-field coupling g — the field itself becomes a dynamical quantity [17] depending on the atomic distribution. As all atoms are coupled to the same field modes, this immediately introduces substantial long range interactions, which cannot be ignored as in free space. In specially designed cases this force induces coherently driven atoms to self-organize in regular patterns as predicted in references [18,19] and subsequently experimentally verified [20].

In addition, in a high-Q optical resonator relatively low photon numbers are sufficient to provide strong forces. This was demonstrated by trapping an atom in the field of just a single photon [21,22]. Hence the inevitable photon number fluctuations induced by cavity damping generate

[a] e-mail: christoph.maschler@uibk.ac.at

force fluctuations on the atoms causing diffusion. At the same time as cavity photon loss constitutes a dissipation channel, it can also carry out energy and entropy of the system. This opens possibilities for cooling of atomic motion [23–26], as demonstrated by beautiful experiments in the group of Rempe [27,28]. Since this cooling mechanism does not require the existence of closed optical cycles it could even be used for qubits [29] or to damp quantum oscillations or phase fluctuations of a BEC coupled to a cavity field [30,31].

For low photon numbers the quantum properties of the light field get important as well and the atoms are now moving in different quantized potentials determined by the cavity photon number. Quantum mechanics of course allows for superpositions of photon numbers invoking superpositions of different optical potentials for the atoms. First simplified models to describe this new physics were recently proposed by us [32] and in parallel by other authors [33]. As the intracavity field itself depends on the atomic state (phase), different atomic quantum states are correlated with different states of the lattice field with differing photon number distributions. In this way quantum mechanics allows for the creation of very exotic atom-field states, like a superposition of a Mott-insulator and superfluid phase, each thereof correlated with a different photon number. Some quite exotic looking phase diagrams for this system were already discussed in reference [33]. Without resorting to the full complex dynamics of the system, the quantum correlations between the field and the atomic wavefunctions open the possibility of non-destructively probing the atomic state by weak scattering of coherent light into the cavity mode [34] and carefully analyzing its properties [35].

It is quite astonishing, that experimental progress in the recent years has made such systems experimentally accessible and at present already several experimental groups succeeded in loading a BEC into a high-Q optical cavity [36–40]. A reliable analysis of these experiments has made more thorough theoretical studies of such systems mandatory.

In this work we concentrate on the study of an ultracold gas in optical lattices including the quantum nature of the lattice potential generated from a cavity field. This extends and substantiates previous studies and predictions on such a system by us [32] as well as other authors [33]. Here we limit ourselves to the case of a high-Q cavity which strongly enhances a field sufficiently red detuned from any atomic transition to induce an optical potential without significant spontaneous emission. In particular we address two different geometric setups, where either the cavity mode is directly driven through one mirror, or the atoms are coherently excited by a transverse laser and scatter light into the cavity mode. The cavity potential can also be additionally enhanced by some extra conservative potential applied at a different frequency [41,42]. These two generic cases leads to quite different physical behavior and allow to discuss several important aspects of the underlying physics.

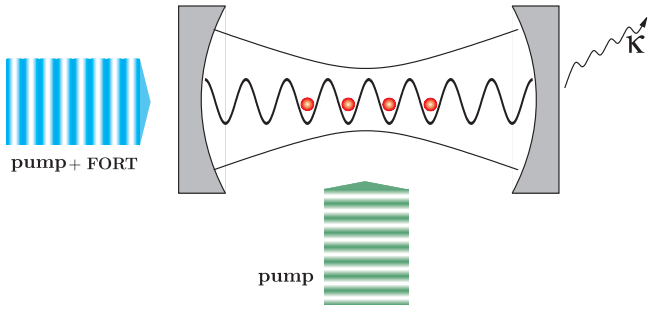

Fig. 1. (Color online) Scheme of atoms inside an optical cavity, driven by two external pumping lasers. An additional conservative lattice potential, independent of the intracavity field, is realized by a far off-resonant dipole trap (FORT).

This paper is organized as follows. Section 2 is devoted to a systematic presentation of our model and various simplifying approximations as adiabatic elimination of the excited states of the atoms and subsequent formulation of an effective multi-particle Hamiltonian in second quantized form. In Section 3, we specialize on the simplest generic case of a coherently driven cavity and approximate the corresponding Hamiltonian by adiabatic elimination of the cavity field. We investigate the properties thereof, corresponding to the influence of the cavity on the Mott-insulator to superfluid quantum phase-transition and identify the regime of validity for the elimination of the cavity field. Finally, we compare these results with the dynamics of the full master equation. In Section 4 we study the more complex case of atoms coherently driven by a laser field transversal to the cavity axis, where it is much harder to find valid analytical simplifications and one has to resort to numerical studies of few particle dynamics. Finally, we conclude in Section 5.

2 Model

We start with N two-level atoms with mass m and transition frequency ω_{eg} strongly interacting with a single standing wave cavity mode of frequency ω_c. We also consider coherent driving of the atoms at frequency ω_p and with maximal coupling strength h_0 and of the cavity with amplitude η (see Fig. 1). Note that in the specific examples later we will consider only one pump laser beam at a time.

Using the rotating-wave and electric-dipole approximation, we can describe a single atom of this system by the Jaynes-Cummings Hamiltonian [43]

$$H^{(1)} = H_A^{(1)} + H_R^{(1)} + H_{Int}^{(1)}. \tag{1}$$

Explicitly the different Hamiltonians for the atoms, the field mode and the interaction read:

$$H_A^{(1)} = \frac{\hat{\mathbf{p}}^2}{2m} + V_e(\mathbf{x})\sigma^+\sigma^- + V_g(\mathbf{x})\sigma^-\sigma^+ + \hbar\omega_{eg}\sigma^+\sigma^- - i\hbar h(\mathbf{x})\left(\sigma^+ e^{-i\omega_p t} - \sigma^- e^{i\omega_p t}\right), \tag{2a}$$

$$H_R^{(1)} = \hbar\omega_c a^\dagger a - i\hbar\eta\left(a e^{i\omega_p t} - a^\dagger e^{-i\omega_p t}\right), \tag{2b}$$

$$H_{Int}^{(1)} = -i\hbar g(\mathbf{x})\left(\sigma^+ a - \sigma^- a^\dagger\right). \tag{2c}$$

Here $h(\mathbf{x})$ denotes the mode-function of the transverse pump field, $g(\mathbf{x})$ denotes the cavity mode function and the field operator a describes the annihilation of a cavity photon with frequency ω_c. $V_e(\mathbf{x})$ and $V_g(\mathbf{x})$ are external trapping potentials for the atom in the excited and the ground state, respectively. In order to change to slowly varying variables we apply a unitary transformation with operator $U(t) = \exp[i\omega_p t\left(\sigma^+\sigma^- + a^\dagger a\right)]$, such that we end up with the following single-particle Hamiltonian, using the same symbols for the transformed quantities:

$$H_A^{(1)} = \frac{\hat{\mathbf{p}}^2}{2m} + V_e(\mathbf{x})\sigma^+\sigma^- + V_g(\mathbf{x})\sigma^-\sigma^+ - \hbar\Delta_a\sigma^+\sigma^- - i\hbar h(\mathbf{x})\left(\sigma^+ - \sigma^-\right), \tag{3a}$$

$$H_R^{(1)} = -\hbar\Delta_c a^\dagger a - i\hbar\eta\left(a - a^\dagger\right), \tag{3b}$$

$$H_{Int}^{(1)} = -i\hbar g(\mathbf{x})\left(\sigma^+ a - \sigma^- a^\dagger\right), \tag{3c}$$

where $\Delta_c = \omega_p - \omega_c$, $\Delta_a = \omega_p - \omega_{eg}$ denotes the detunings of the cavity and the atomic transition frequency from the pumping field frequency. In order to describe the situation for N atoms, we use the single-particle Hamiltonian of equations (1) and (3) in second quantization formalism [44], i.e.,

$$H = H_A + H_R + H_{A-R} + H_{A-P} + H_{A-A}. \tag{4}$$

The terms in this expression correspond to the single particle terms in (2) and (3). Hence, H_A and H_R model the free evolution of the atomic and the field variables, respectively. They read as:

$$H_A = \int d^3\mathbf{x}\left[\Psi_g^\dagger(\mathbf{x})\left(-\frac{\hbar^2}{2m}\nabla^2 + V_g(\mathbf{x})\right)\Psi_g(\mathbf{x}) + \Psi_e^\dagger(\mathbf{x})\left(-\frac{\hbar^2}{2m}\nabla^2 - \hbar\Delta_a + V_e(\mathbf{x})\right)\Psi_e(\mathbf{x})\right], \tag{5}$$

where $\Psi_g(\mathbf{x})$ and $\Psi_e(\mathbf{x})$ denotes the atomic field operators for annihilating an atom at position $\mathbf{x}$ in the ground state and the excited state, respectively. They obey the usual bosonic commutation relations

$$\left[\Psi_f(\mathbf{x}), \Psi_{f'}^\dagger(\mathbf{x}')\right] = \delta^3\left(\mathbf{x} - \mathbf{x}'\right)\delta_{f,f'} \tag{6a}$$

$$\left[\Psi_f(\mathbf{x}), \Psi_{f'}(\mathbf{x}')\right] = \left[\Psi_f^\dagger(\mathbf{x}), \Psi_{f'}^\dagger(\mathbf{x}')\right] = 0, \tag{6b}$$

for $f, f' \in \{e, g\}$. The field operator remains unchanged, i.e., $H_R = -\hbar\Delta_c a^\dagger a - i\hbar\eta\left(a - a^\dagger\right)$. The two-body interaction is modeled by a short-range pseudopotential [45], characterized by the s-wave scattering length a_s, leading to a Hamiltonian

$$H_{A-A} = \frac{U}{2}\int d^3\mathbf{x}\Psi_g^\dagger(\mathbf{x})\Psi_g^\dagger(\mathbf{x})\Psi_g(\mathbf{x})\Psi_g(\mathbf{x}), \tag{7}$$

where $U = 4\pi a_s\hbar^2/m$. The coupling of the cavity field with the atoms inside the cavity is given by

$$H_{A-R} = -i\hbar\int d^3\mathbf{x}\Psi_g^\dagger(\mathbf{x})g(\mathbf{x})a^\dagger\Psi_e(\mathbf{x}) + \text{h.c.}, \tag{8}$$

whereas the interaction with the laser beam, which coherently drives the atoms, reads

$$H_{A-P} = -i\hbar\int d^3\mathbf{x}\Psi_g^\dagger(\mathbf{x})h(\mathbf{x})\Psi_e(\mathbf{x}) + \text{h.c.} \tag{9}$$

Let us now calculate the Heisenberg equations for the various field operators, starting with the operator for the excited state, i.e.,

$$\frac{\partial\Psi_e(\mathbf{x})}{\partial t} = i\left[\frac{\hbar}{2m}\nabla^2 - \frac{V_e(\mathbf{x})}{\hbar} + \Delta_a\right]\Psi_e(\mathbf{x}) - \left[g(\mathbf{x})\,a + h(\mathbf{x})\right]\Psi_g(\mathbf{x}). \tag{10}$$

The first term corresponds to the free evolution of the atomic state, whereas the second term describes the absorption of a cavity photon or a pump photon together with the annihilation of a ground state atom. Similarly, the equation for the ground state operator reads:

$$\frac{\partial\Psi_g(\mathbf{x})}{\partial t} = i\left[\frac{\hbar}{2m}\nabla^2 - \frac{V_g(\mathbf{x})}{\hbar} - \frac{U}{\hbar}\Psi_g^\dagger(\mathbf{x})\Psi_g(\mathbf{x})\right]\Psi_g(\mathbf{x}) + \left[g(\mathbf{x})\,a^\dagger + h(\mathbf{x})\right]\Psi_e(\mathbf{x}). \tag{11}$$

Finally, the Heisenberg equation for the cavity field operator is given by:

$$\frac{\partial a}{\partial t} = i\Delta_c a + \eta + \int d^3\mathbf{x}g(\mathbf{x})\Psi_g^\dagger(\mathbf{x})\Psi_e(\mathbf{x}). \tag{12}$$

Again, the first term corresponds to the free field evolution, whereas the last two terms are driving terms of the cavity field.

As we want to treat temperatures close to $T = 0$ we have to avoid heating and ensure weak atomic excitation, where there is only negligible spontaneous emission. In this limit we can adiabatically eliminate the excited states from the dynamics of our system. This requires large atom-pump detunings Δ_a, where we also can neglect the kinetic energy term and the trapping potential in (10) compared to Δ_a. Necessarily, we assume that the field operators $\Psi_g(\mathbf{x})$ and a vary on a much slower time scale than the $1/\Delta_a$ terms, such that we obtain:

$$\Psi_e(\mathbf{x}, t) = -\frac{i}{\Delta_a}\left[h(\mathbf{x}) + g(\mathbf{x})a(t)\right]\Psi_g(\mathbf{x}, t). \tag{13}$$

Inserting this expression for $\Psi_e(\mathbf{x})$ into (11) and (12) leads then to:

$$\frac{\partial\Psi_g(\mathbf{x})}{\partial t} = i\left[\frac{\hbar}{2m}\nabla^2 - \frac{V_g(\mathbf{x})}{\hbar} - \frac{h^2(\mathbf{x})}{\Delta_a} - \frac{g^2(\mathbf{x})}{\Delta_a}a^\dagger a - \frac{h(\mathbf{x})g(\mathbf{x})}{\Delta_a}\left(a + a^\dagger\right) - \frac{U}{\hbar}\Psi_g^\dagger(\mathbf{x})\Psi_g(\mathbf{x})\right]\Psi_g(\mathbf{x}), \tag{14}$$

$$\frac{\partial a}{\partial t} = i\left[\Delta_c - \frac{1}{\Delta_a}\int d^3\mathbf{x}g^2(\mathbf{x})\Psi_g^\dagger(\mathbf{x})\Psi_g(\mathbf{x})\right]a - \frac{i}{\Delta_a}\int d^3\mathbf{x}h(\mathbf{x})\Psi_g^\dagger(\mathbf{x})\Psi_g(\mathbf{x}) + \eta. \tag{15}$$

To discuss the underlying physics in a tractable form, the trick is now to find an effective Hamiltonian $H_{\rm eff}$ which leads to the same dynamics as given by equations (14) and (15). Thus this Hamiltonian has to obey:

$$i\hbar\frac{\partial\Psi_g(\mathbf{x})}{\partial t} = [\Psi_g(\mathbf{x}), H_{\rm eff}] \quad \text{and} \quad i\hbar\frac{\partial a}{\partial t} = [a, H_{\rm eff}]. \tag{16}$$

From this we can easily read off a possible effective Hamiltonian of the form:

$$\begin{aligned} H_{\rm eff} = \int d^3\mathbf{x}\Psi_g^\dagger(\mathbf{x}) \Big\{ -\frac{\hbar^2}{2m}\nabla^2 + V_g(\mathbf{x}) \\ + \frac{\hbar}{\Delta_a}\left[h^2(\mathbf{x}) + g^2(\mathbf{x})a^\dagger a + h(\mathbf{x})g(\mathbf{x})\left(a + a^\dagger\right)\right]\Big\}\Psi_g(\mathbf{x}) \\ + \frac{U}{2}\int d^3\mathbf{x}\Psi_g^\dagger(\mathbf{x})\Psi_g^\dagger(\mathbf{x})\Psi_g(\mathbf{x})\Psi_g(\mathbf{x}) \\ - i\hbar\eta\left(a - a^\dagger\right) - \hbar\Delta_c a^\dagger a. \end{aligned} \tag{17}$$

The corresponding single particle Hamiltonian, which leads to this second quantized Hamiltonian is[1]

$$\begin{aligned} H_{\rm eff}^{(1)} = \frac{\mathbf{p}^2}{2m} + V_g(\mathbf{x}) + \frac{\hbar}{\Delta_a}\left[h^2(\mathbf{x}) + g^2(\mathbf{x})a^\dagger a \right. \\ \left. + h(\mathbf{x})g(\mathbf{x})\left(a + a^\dagger\right)\right] - i\hbar\eta\left(a - a^\dagger\right) - \hbar\Delta_c a^\dagger a. \end{aligned} \tag{18}$$

This simplified effective atom-field Hamiltonian will be the basis of our further considerations. It is, however, still much too complex for a general solution and we will have to make further simplifying assumptions. Hence at this point we will restrict ourselves to 1D motion along the cavity axis. In an experimental setup this could be actually realized by a deep radial trapping potential, but we think that at least qualitatively the model should also capture the essential physics if some transverse motion of the particles was allowed. As one consequence this assumption requires a rescaling of the effective two-body interaction strength [46], which enters as a free parameter in our model anyway.

Mathematically we thus end up with a one-dimensional optical lattice, which is partly generated by the resonator field and superimposed onto a prescribed extra trapping potential $V_g(\mathbf{x}) = V_g(x)$. The mode function of the cavity along the axis is approximated by $g(\mathbf{x}) = g(x) = g_0\cos(kx)$ and the transverse laser beam forms a broad standing wave $h(\mathbf{x}) = h_0\cos(k_p y)$, which in our one-dimensional considerations ($y = 0$) is just a constant term that we can eventually omit in (17).

As we consider external pumping of atoms and mode, we essentially treat an open system and we have to deal with dissipation as well. Such dissipation processes are modeled by Liouvillean terms $\mathcal{L}$ appearing in the master equation for the atom-field density operator, i.e.,

$$\dot{\varrho} = \frac{1}{i\hbar}[H_{\rm eff}, \varrho] + \mathcal{L}\varrho. \tag{19}$$

[1] It is also possible, first to eliminate the excited state in the single particle dynamics, which leads to the same expression (18) and then implement this expression in second quantization formalism.

As mentioned above, we assume large atom-pump detuning Δ_a, suppressing spontaneous emission to a large extend. However, we still have to deal with the cavity loss κ, which will thus be the dominant dissipation process. Hence the corresponding Liouvillean using a standard quantum optics approach [49] reads:

$$\mathcal{L}\varrho = \kappa\left(2a\varrho a^\dagger - a^\dagger a\varrho - \varrho a^\dagger a\right). \tag{20}$$

Equivalently in the corresponding Heisenberg equation for the field operator, cavity loss leads to damping terms and fluctuations, so that it then reads:

$$\begin{aligned} \dot{a} = \left\{ i\left[\Delta_c - \frac{g_0^2}{\Delta_a}\int dx\Psi_g^\dagger(x)\cos^2(kx)\Psi_g(x)\right] - \kappa\right\} a \\ - i\frac{g_0 h_0}{\Delta_a}\int dx\Psi_g^\dagger(x)\cos(kx)\Psi_g(x) + \eta + \Gamma_{in}. \end{aligned} \tag{21}$$

Since we will be mainly interested in normally ordered quantities and assume vacuum ($T = 0$) outside the cavity, the input noise operators Γ_{in} will not enter in the dynamics, such that we will omit them later.

Let us now proceed and transform the Hamiltonian into a more commonly known form. Following standard procedures, one constructs maximally localized eigenfunctions at each site and expands the atomic field operator $\Psi_g(x)$ in terms of single atom Wannier functions [48]

$$\Psi_g(x) = \sum_n\sum_k b_{n,k}w_n(x - x_k), \tag{22}$$

where $b_{n,k}$ corresponds to the annihilation of a particle in the $n-$th energy band at site k. Since we assume the involved energies to be much smaller than the excitation energies to the second band, we are able to keep only the lowest vibrational state in the Wannier expansion, i.e., $\Psi_g(x) = \sum_k b_k w(x - x_k)$, where $w(x) = w_0(x)$. This yields to the following Hamiltonian:

$$\begin{aligned} H = \sum_{k,l} E_{kl}b_k^\dagger b_l + \left(\hbar U_0 a^\dagger a + V_{\rm cl}\right)\sum_{k,l} J_{kl}b_k^\dagger b_l \\ + \hbar\eta_{\rm eff}\left(a + a^\dagger\right)\sum_{k,l}\tilde{J}_{kl}b_k^\dagger b_l - i\hbar\eta\left(a - a^\dagger\right) \\ + \frac{1}{2}\sum_{i,j,k,l} U_{ijkl}b_i^\dagger b_j^\dagger b_k b_l - \hbar\Delta_c a^\dagger a, \end{aligned} \tag{23}$$

where the addendum *eff* of the Hamiltonian is omitted. Here we introduced an important characteristic parameter of atomic cavity QED, namely the refractive index U_0 of a single atom at an antinode, which is given by $U_0 = g_0^2/\Delta_a$. It gives the frequency shift of the cavity mode induced by a single atom at an antinode and also corresponds to the optical lattice depth for an atom per cavity photon [17]. Similarly, the parameter $\eta_{\rm eff} = g_0 h_0/\Delta_a$ describes the position dependent effective pump strength of the cavity mode induced by the scattered light from a single atom at an antinode.

Note that the Wannier state expansion equation (22) depends on the potential depth. Thus the Wannier functions and the corresponding matrix elements depend on

the cavity field and thus in principle are dynamic quantities. However, they keep the same functional form with a few changing parameters, which have to be determined consistently. This is of course consequently also true for the various coupling parameters in the Hamiltonian. The above model thus can only be valid as long as the single band approximation stays valid during the system dynamics and the parameters don't change to rapidly. In the special but rather interesting case, where the atoms are trapped solely by the cavity field [21,22] this is not valid for very low photon numbers. Here a single photon number jump will induce excitation to higher bands, which induces nonlinear dynamics beyond the single band model.

In practice this problem can be circumvented by adding an additional external trapping potential $V_g(x)$ to the model, which guarantees a minimum potential depth even in the case of zero cavity photons. Experimentally this is feasible, for instance, with a far detuned, off-resonant dipole trap (FORT) [50], i.e., $V_g(x) = V_{\rm cl}\cos^2(k_F x)$, where k_F denotes the wave number of the FORT field. In the experimental realization, the frequency of the corresponding laser field ω_F is only very few free spectral ranges separated from the main cavity frequency ω_c [27,51,52]. Hence, in the vicinity of the cavity center, the coincidence of the FORT field and the cavity field is very good, and we can replace in good agreement $\cos^2(k_F x)$ with $\cos^2(kx)$.

Let us remark here that by including this extra potential, we can keep our model and allow for further analytical analysis of the dynamics, but we also have thrown out a great deal of interesting physics already. Actually, for very few atoms one still can solve the full Hamiltonian without the restriction to the lowest bands by quantum Monte Carlo wavefunction simulations. Some early results of such simulations can be found in references [55,56]. However, this is not the subject of this work and we will proceed here with the effective lattice model under the assumption of a deep enough extra potential or strong enough cavity fields.

Note that in (23), in contrast to the case of the Bose-Hubbard model in a classical optical lattice, where the matrix elements of the potential and kinetic energy can be merged, here two separate parts exist due to the presence of the cavity field operators in the Hamiltonian. Explicitly they read as:

$$E_{kl} = \int dx\, w(x-x_k)\left(-\frac{\hbar^2}{2m}\nabla^2\right) w(x-x_l), \tag{24a}$$

$$J_{kl} = \int dx\, w(x-x_k)\cos^2(kx) w(x-x_l), \tag{24b}$$

$$\tilde{J}_{kl} = \int dx\, w(x-x_k)\cos(kx) w(x-x_l). \tag{24c}$$

The on-site elements J_{kk} and E_{kk} are independent of the lattice site k, whereas $\tilde{J}_{kl}$ changes sign periodically, i.e., $\tilde{J}_{kk} = -\tilde{J}_{k+1,k+1}$ due to the cos, which has twice the periodicity of the lattice. This also accounts for $\tilde{J}_{k,k+1} = 0$. Note that the existence of this term implies that two adjacent wells acquire different depths forcing us to reassure that for the case of the directly pumped atom $\eta_{\rm eff}(a+a^\dagger)\cos(kx)$ is only a small perturbation of the lattice. As the next-nearest elements are typically two orders of magnitude smaller than the nearest-neighbor term [3] they can safely be neglected (tight-binding approximation). Hence we label the site-independent on-site matrix elements with E_0, J_0 and $\tilde{J}_0$, whereas E and J are the site-to-site hopping elements. Furthermore, in the case of the nonlinear interaction matrix elements,

$$U_{ijkl} = g_{1D}\int dx w(x-x_i)w(x-x_j)w(x-x_k)w(x-x_l), \tag{25}$$

we can omit the off-site terms since they are also typically two orders of magnitude smaller than the on-site interaction matrix elements. Note that g_{1D} is the one-dimensional on-site interaction strength, originating from an adjustment of the scattering length a_s, due to the transversal trapping [46]. As a central result of our studies we therefore obtain a generalized Bose-Hubbard Hamiltonian:

$$\begin{aligned} H = {} & E_0\hat{N} + E\hat{B} + \left(\hbar U_0 a^\dagger a + V_{\rm cl}\right)\left(J_0\hat{N} + J\hat{B}\right) \\ & + \hbar\eta_{\rm eff}\left(a+a^\dagger\right)\tilde{J}_0\sum_k(-1)^{k+1}\hat{n}_k - \hbar\Delta_c a^\dagger a \\ & - i\hbar\eta\left(a-a^\dagger\right) + \frac{U}{2}\sum_k \hat{n}_k\left(\hat{n}_k - 1\right), \end{aligned} \tag{26}$$

where the nonlinear on-site interaction is characterized by $U = g_{1D}\int dx\,|w(x)|^4$. In addition, we introduced the number operator $\hat{N} = \sum_k \hat{n}_k = \sum_k b_k^\dagger b_k$ and the jump operator $\hat{B} = \sum_k\left(b_{k+1}^\dagger b_k + \text{h.c.}\right)$. Note that for strong classical intracavity fields and no transverse pump we recover the standard Bose-Hubbard Hamiltonian.

Finally, let us remark that we now can also rewrite the field Heisenberg equation (21) in the above terms, which gives:

$$\begin{aligned} \dot{a} = {} & \left\{i\left[\Delta_c - U_0\left(J_0\hat{N} + J\hat{B}\right)\right] - \kappa\right\}a + \eta \\ & - i\eta_{\rm eff}\tilde{J}_0\sum_k(-1)^{k+1}\hat{n}_k. \end{aligned} \tag{27}$$

Here we clearly see that besides the number operator $\hat{N}$ for the atoms also the coherence properties via the operator $\hat{B}$ and statistics via $\hat{n}_k$ play a decisive role in the field dynamics. As this field acts back on the atomic motion, interesting and complex coupled dynamics can be expected from this model, which was partly already discussed in [32,33] and will be elucidated more in the remainder of this work.

3 Cavity pump

Let us now turn to the conceptually simplest case and restrict the pumping only to the cavity, where only a single mode is coherently excited (*cavity pumping*). This mode

will generate an optical potential in addition to the prescribed external potential. For large enough photon numbers the external potential can even be omitted and the particles are trapped solely by the cavity field. As essential ingredient in the dynamics, the identical coupling of all atoms to this same field mode induces a long-range interaction between the atoms independent of their positions. Setting $\eta_{\rm eff}=0$, the Hamiltonian (26) is reduced to:

$$H = E_0\hat{N} + E\hat{B} + \left(\hbar U_0 a^\dagger a + V_{\rm cl}\right)\left(J_0\hat{N} + J\hat{B}\right) - \hbar\Delta_c a^\dagger a - i\hbar\eta\left(a - a^\dagger\right) + \frac{U}{2}\hat{C}. \quad (28)$$

Here we introduced $\hat{C} = \sum_k \hat{n}_k\left(\hat{n}_k - 1\right)$ for the operator of the two-body on-site interaction. Still we see that the corresponding Heisenberg equation for the cavity field:

$$\dot{a} = \left\{i\left[\Delta_c - U_0\left(J_0\hat{N} + J\hat{B}\right)\right] - \kappa\right\}a + \eta \quad (29)$$

depends on atom number and coherence. For very weak fields this yields an atom statistics dependent cavity transmission spectrum, which was studied in some detail in reference [35]. Here we go one step further and study the dynamical back action of the field onto atomic motion and field mediated atom-atom interaction, which appear at higher photon number. As the model is still rather complex we need some further approximations at this point in order to catch some qualitative insight.

3.1 Field-eliminated Hamiltonian

Although the influence of the cavity field on the atoms is equal on all particles, their common interaction generates a dynamics much more complex than for a Bose-Hubbard model with prescribed external potential. This is more analogous to real solid state physics where the state of the electrons also acts back on the potentials. To exhibit the underlying physics, we will now derive an approximate Hamiltonian, which solely depends on particle variables by adiabatically eliminating the field (28). This should be valid when the damping rate κ of the cavity generates a faster time scale than the external atomic degrees of freedom. Actually as tunneling is mostly a very slow process (much slower than the recoil frequency), this will be almost always the case in practical experimental setups. To this end, we simply equate (29) to zero and obtain formally $a = \eta/\{\kappa - i[\Delta_c - U_0(J_0\hat{N} + J\hat{B})]\}$. In the following we constrain ourselves to the case of a fixed number of atoms, i.e., $\hat{N} = N\mathbf{1}$. The very small tunneling matrix element J can be used as an expansion parameter, leading to:

$$a \approx \frac{\eta}{\kappa - i\Delta_c'}\left[\mathbf{1} - i\frac{U_0 J}{\kappa - i\Delta_c'}\hat{B} - \frac{(U_0 J)^2}{(\kappa - i\Delta_c')^2}\hat{B}^2\right], \quad (30)$$

where we introduced a shifted detuning $\Delta_c' = \Delta_c - U_0 J_0 N$.

In order to obtain an effective Hamiltonian, where the cavity degrees of freedom are eliminated, we replace the field terms in (28), by the steady state expressions (30), as well as in the Liouville super operator (20). Note, that this is more appropriate than the naive approach of a replacement just in the Hamiltonian, as has been done in our former work [32]. If we consider terms up to order $\propto J^2$, the exchange in the Hamiltonian yields:

$$H_{\rm ad} = (E + JV_{\rm cl})\hat{B} + \frac{U}{2}\hat{C} + \frac{\hbar U_0 J\eta^2}{\kappa^2 + {\Delta_c'}^2}\left(\frac{{\Delta_c'}^2 - \kappa^2}{\kappa^2 + {\Delta_c'}^2}\hat{B} - \frac{3U_0 J\Delta_c'}{\kappa^2 + {\Delta_c'}^2}\hat{B}^2\right). \quad (31)$$

Next, by applying the same procedure to the Liouville equation – again up to terms $\propto J^2$ – we obtain an adiabatic Liouville operator:

$$\mathcal{L}_{\rm ad}\varrho = -i\frac{2U_0 J\kappa^2\eta^2}{\left(\kappa^2 + {\Delta_c'}^2\right)^2}\left[\hat{B} + \frac{2\Delta_c' U_0 J}{\kappa^2 + {\Delta_c'}^2}\hat{B}^2, \varrho\right] + \frac{\kappa U_0^2 J^2\eta^2}{\left(\kappa^2 + {\Delta_c'}^2\right)^2}\left(2\hat{B}\varrho\hat{B} - \hat{B}^2\varrho - \varrho\hat{B}^2\right). \quad (32)$$

The Lindblad terms in the second line are real, corresponding to dissipation, whereas the first, imaginary term corresponds to a unitary time evolution and has therefore to be added to the adiabatic Hamiltonian, i.e.,

$$H_{\rm ad} \to H_{\rm ad} + \frac{2\hbar U_0 J\kappa^2\eta^2}{\left(\kappa^2 + {\Delta_c'}^2\right)^2}\left(\hat{B} + \frac{2\Delta_c' U_0 J}{\kappa^2 + {\Delta_c'}^2}\hat{B}^2\right).$$

Altogether, we end up with a Hamiltonian, where the cavity field has been eliminated:

$$H_{\rm ad} = (E + JV_{\rm cl})\hat{B} + \frac{U}{2}\hat{C} + \frac{\hbar U_0 J\eta^2}{\kappa^2 + {\Delta_c'}^2}\left(\hat{B} + \frac{U_0 J\Delta_c'}{\kappa^2 + {\Delta_c'}^2}\frac{\kappa^2 - 3{\Delta_c'}^2}{\kappa^2 + {\Delta_c'}^2}\hat{B}^2\right). \quad (33)$$

The loss rate of the cavity is described by the remaining dissipative part of (32):

$$\mathcal{L}_{\rm ad}\varrho = \frac{\kappa U_0^2 J^2\eta^2}{\left(\kappa^2 + {\Delta_c'}^2\right)^2}\left(2\hat{B}\varrho\hat{B} - \hat{B}^2\varrho - \varrho\hat{B}^2\right). \quad (34)$$

Note, that the above adiabatic elimination procedure is not completely unambiguous due to ordering freedom. Nevertheless it should give a qualitatively correct first insight. An alternative way of deriving an effective Hamiltonian, depending solely on particle observable is similar to (16) and (17). This amounts to a replacement of the field variables with (30) in the Heisenberg equation for the external atomic degrees of freedom, which read as follows:

$$\dot{b}_k = \frac{1}{i\hbar}\left[\left(E + JV_{cl} + \hbar U_0 J a^\dagger a\right)\left(b_{k-1} + b_{k+1}\right) - U\hat{n}_k b_k\right]. \quad (35)$$

A naive replacement of the field operator a and its adjoint $a^\dagger$ by (30) in the above expression leads to an equation for

$\dot{b}_k$, which cannot be generated from an effective adiabatic Hamiltonian in the form $\dot{b}_k = -i/\hbar[b_k, H_{\rm ad}]$. Hence, before substituting the adiabatic field operators, we have to symmetrize the expression containing the field term in (35) in the form

$$\dot{b}_k = -\frac{i}{\hbar}\left[(E + JV_{cl})\left(b_{k-1} + b_{k+1}\right) - U\hat{n}_k b_k\right] - \frac{i\hbar U_0 J}{2}\left[a^\dagger a\left(b_{k-1} + b_{k+1}\right) + \left(b_{k-1} + b_{k+1}\right)a^\dagger a\right]. \quad (36)$$

This form enables us to describe the dynamics of b_k by a Heisenberg equation with an effective Hamiltonian, which up to second order in J reads:

$$H_{\rm ad} = (E + JV_{\rm cl})\hat{B} + \frac{U}{2}\hat{C} + \frac{\hbar U_0 J\eta^2}{\kappa^2 + {\Delta'_c}^2}\left(\hat{B} + \frac{U_0 J\Delta'_c}{\kappa^2 + {\Delta'_c}^2}\hat{B}^2\right). \quad (37)$$

The terms in the second line stem from the field terms in (36). Although this Hamiltonian looks a bit different from the first version derived before (33), their properties are – within their regime of validity – in very good agreement as long as hopping is slow compared to damping.

To exhibit the physical content of this Hamiltonian one can look at its eigenstates. As first step we calculate the Mott insulator state (see Eq. (49)) fraction of the lowest energy state $|\psi\rangle$ of these two Hamiltonians, i.e., $p_{\rm MI} = |\langle\psi|{\rm MI}\rangle|^2$ (see also Fig. 4), as a function of the on-site interaction energy for different values of Δ'_c. This will indicate changes of position and behavior of the Mott insulator superfluid transition (see Fig. 4). To compare the two approximate Hamiltonians in Figure 2, we plot the difference of the Mott insulator fraction of the ground state of (33) and (37), as well as the difference of the steady state photon number. Obviously the two Hamiltonians, converge in the limit of large cavity decay κ. This can also be seen in Figure 2, where the dashed-dotted line depicts the case of a smaller Δ'_c (which is equivalent to an enlarged κ), showing a strongly enhanced coincidence.

3.2 Field-eliminated density operator

Let us now use a further and somehow more systematic alternative approach to eliminate the cavity field dynamics from the system evolution directly from the Liouville equation by following a method proposed by Wiseman and Milburn [53], which is valid for large κ and low photon numbers. In this case we have

$$\left|\frac{\langle H_{at}\rangle}{\kappa}\right| \sim \left|\frac{\hbar U_0\langle a^\dagger a\rangle}{\kappa}\right| = \varepsilon \ll 1, \quad (38)$$

where H_{at} is the atomic part of (28), i.e., $H_{at} = (E + V_{cl}J)\,\hat{B} + U\hat{C}/2$. Again the total atom number $\hat{N}$ is supposed to be constant. This allows to expand the density operator in powers of ε, corresponding to states with increasing photon number:

$$\varrho = \varrho_0 \otimes |0\rangle_a\langle 0| + (\varrho_1 \otimes |1\rangle_a\langle 0| + h.c.) + \varrho_2 \otimes |1\rangle_a\langle 1| + (\varrho'_2 \otimes |2\rangle_a\langle 0| + h.c.) + O\left(\varepsilon^3\right). \quad (39)$$

Here ϱ_i are density operators for the particle variables, corresponding to the order i of magnitude in the expansion parameter ε. We substitute this expression into the

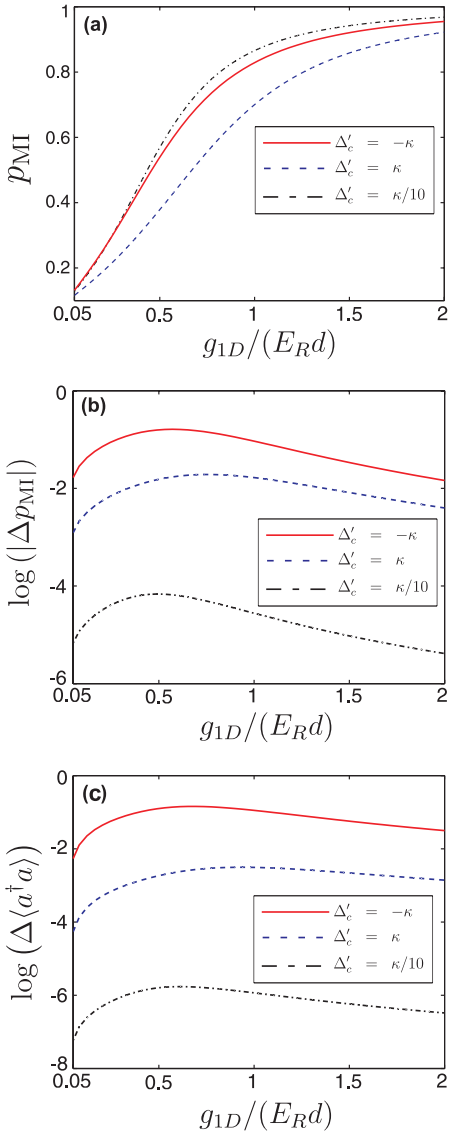

Fig. 2. (Color online) (a) Contribution of the Mott-insulator state to the ground state $p_{\rm MI} = |\langle\psi|{\rm MI}\rangle|^2$ of (37) as function of the 1D on-site interaction strength in units of $E_R d$ (d is the lattice constant). (b) Logarithmic difference of $p_{\rm MI}$, calculated with the groundstate of (37) and (33). (c) Logarithmic difference of the adiabatically eliminated photon number $\langle\psi|a^\dagger a|\psi\rangle$ with a from (30) for the two different ground states. The parameters are $\kappa = 1/\sqrt{2}\omega_R, \eta = 2.35\ \omega_R$ and $\Delta'_c = -\kappa$ (red, solid line), $\kappa = 4\omega_R, \eta = 12.5\omega_R$ and $\Delta'_c = \kappa$ (blue, dashed line) and $\kappa = 4\omega_R, \eta = 10\omega_R$ and $\Delta'_c = -\kappa/10$ (black, dashed-dotted line). In any of the curves, we set $V_{\rm cl} = 0$ and $U_0 = -\omega_R$. Here ω_R is the frequency corresponding to the recoil energy, i.e., $E_R = \hbar^2k^2/(2m) = \hbar\omega_R$.

Liouville equation (19) with the Hamiltonian from (28), which leads to the following set of equations:

$$\dot{\varrho}_0 = \frac{1}{i\hbar}[H_{at}, \varrho_0] - \eta\left(\varrho_1 + \varrho_1^\dagger\right) + 2\kappa\varrho_2 \tag{40a}$$

$$\dot{\varrho}_1 = \frac{1}{i\hbar}[H_{at}, \varrho_1] - \eta\left(\sqrt{2}\varrho_2' + \varrho_2 - \varrho_0\right) - \kappa\varrho_1 + i\left[\Delta_c - U_0\left(J_0 N + J\hat{B}\right)\right]\varrho_1 + \kappa O\left(\varepsilon^4\right) \tag{40b}$$

$$\dot{\varrho}_2 = \frac{1}{i\hbar}[H_{at}, \varrho_2] + \eta\left(\varrho_1 + \varrho_1^\dagger\right) - 2\kappa\varrho_2 - iU_0\left[J_0 N + J\hat{B}, \varrho_2\right] + \kappa O\left(\varepsilon^4\right) \tag{40c}$$

$$\dot{\varrho}_2' = \frac{1}{i\hbar}[H_{at}, \varrho_2'] + \sqrt{2}\eta\varrho_1 - 2\kappa\varrho_2' + 2i\left[\Delta_c - U_0\left(J_0 N + J\hat{B}\right)\right]\varrho_2' + \kappa O\left(\varepsilon^4\right). \tag{40d}$$

Now we adiabatically eliminate the off-diagonal elements ϱ_1 and ϱ_2'. Setting their derivations in (40b) and (40d) to zero and neglecting terms with respect to the assumption (38), we obtain:

$$\varrho_2' = \frac{\eta}{\sqrt{2}A}\varrho_1 + O\left(\varepsilon^3\right). \tag{41}$$

This is consistent with the assumption $\varrho_2' \sim O\left(\varepsilon^2\right)$. Here we defined $A = \kappa - i\Delta_c' + iU_0 J\hat{B}$. Putting (41) into (40b) and neglecting the terms consistent with the order of the expansion, such that $\varrho_1 \sim O\left(\varepsilon\right)$, it follows that:

$$\varrho_1 = \frac{\eta}{A + \eta^2/A}\left(\varrho_0 - \varrho_2\right) + O\left(\varepsilon^4\right). \tag{42}$$

We simplify this expression, $\varrho_1 \approx \eta A^{-1}(\varrho_0 - \varrho_2)$, which is consistent with the above expansion and substitute it into (40a) and (40c):

$$\dot{\varrho}_0 = \frac{1}{i\hbar}[H_{at}, \varrho_0] + 2\kappa\varrho_2 - \eta^2\left[A^{-1}\left(\varrho_0 - \varrho_2\right) + \left(\varrho_0 - \varrho_2\right)A^{\dagger\,-1}\right], \tag{43a}$$

$$\dot{\varrho}_2 = \frac{1}{i\hbar}[H_{at}, \varrho_2] - iU_0\left[J_0 N + J\hat{B}, \varrho_2\right] - 2\kappa\varrho_2 + \eta^2\left[A^{-1}\left(\varrho_0 - \varrho_2\right) + \left(\varrho_0 - \varrho_2\right)A^{\dagger\,-1}\right]. \tag{43b}$$

In order to formulate a master equation for the particle variables we have to use the reduced density operator, where we trace over the field variables, i.e., $\varrho_{at} = \mathrm{tr}(\varrho) = \varrho_0 + \varrho_2 + O\left(\varepsilon^4\right)$. With (43a) and (43b) we see that:

$$\dot{\varrho}_{at} = \frac{1}{i\hbar}[H_{at}, \varrho_{at}] - iU_0\left[J_0 N + J\hat{B}, \varrho_2\right]. \tag{44}$$

As a further approximation, which is also consistent with the expansion order of the assumption (38), we set (43b) to zero and neglect $[H_{at}, \varrho_2]$ and all other terms smaller than $O\left(\varepsilon^3\right)$. Then we can express ϱ_2 through ϱ_0:

$$\varrho_2 = \frac{\eta^2}{2\kappa}\left[A^{-1}\varrho_0 + \varrho_0 A^{\dagger\,-1}\right]. \tag{45}$$

Within this order of magnitude of ε we can replace ϱ_0 with ϱ_{at}, leading us finally to the following master equation for the reduced density operator of the particle variables:

$$\dot{\varrho}_{at} = \frac{1}{i\hbar}[H_{at}, \varrho_{at}] - i\frac{U_0\eta^2}{2\kappa}\left[J_0 N + J\hat{B}, \left(A^{-1}\varrho_{at} + \varrho_{at}A^{\dagger\,-1}\right)\right]. \tag{46}$$

Note that this model also contains a damping part, since the operator A is not hermitian. Let us investigate this damping, by expanding the inverse of A up to first order in J, which is consistent with the order of magnitude in (46). Hence we replace A^{-1} and its adjoint in this equation by

$$A^{-1} \approx \frac{1}{\kappa - i\Delta_c'}\left(1 - i\frac{U_0 J}{\kappa - i\Delta_c'}\hat{B}\right) \tag{47}$$

and its adjoint. Since we are restricted on a subspace of constant atom number, the Liouville equation reads as follows:

$$\dot{\varrho}_{at} = \frac{1}{i\hbar}\left[H_{at} + \frac{\hbar U_0\eta^2}{\kappa^2 + \Delta_c'^{\,2}}\left(J\hat{B} + \frac{U_0\Delta_c' J^2}{\kappa^2 + \Delta_c'^{\,2}}\hat{B}^2\right), \varrho_{at}\right] - \frac{(JU_0\eta)^2}{2\kappa}\frac{\kappa^2 - \Delta_c'^{\,2}}{\left(\kappa^2 + \Delta_c'^{\,2}\right)^2}\left[\hat{B}, \left[\hat{B}, \varrho_{at}\right]\right]. \tag{48}$$

Obviously, the non-dissipative part of this equation agrees perfectly with our adiabatically eliminated Hamiltonian (37) and the structure of the dissipative part is of the same Lindblad form as (34). Note that an expansion of A^{-1} to higher order in J would also provide us the correct next-order term of (37) plus an extra term in the Liouville-equation, which does not correspond to unitary time evolution, as described by a Hamiltonian. This confirms the usefulness of the naive elimination method, also used in reference [32].

3.3 Quantum phase transitions in an optical lattice

In Section 3.1 we derived two approximate Hamiltonians (33) and (37) describing our system of cold atoms in an optical lattice. To a large extend they still implement the well-known BH model, but with parameters controllable via cavity detuning and some additional nonlocal interaction terms. Let us now investigate their properties in some more detail. One of the key features of optical cavities is the feedback mechanism between atoms and cavity field. Hence, computations are a subtle issue, since the matrix elements in the BH Hamiltonian depend on the field amplitude, which itself depends on the atomic positions. In principle a rigorous treatment would consist of calculating the matrix elements (24) for every photon Fock state and treating the parameters of the BH model as operators. To avoid the full complexity of such an approach we will first assume only a weak dependence of the Wannier functions on the mean cavity photon number $\langle a^\dagger a\rangle$, which allows us to proceed analytically. For any set of operating parameters

Highlight Paper

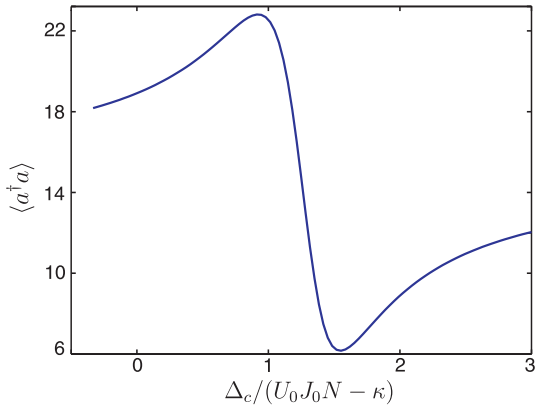

Fig. 3. Self-consistent photon number in the case of four particles in four wells without on-site interaction. Parameters are $U_0 = -\omega_R$ and $\kappa = \omega_R$.

we then calculate the matrix elements in a self-consistent way replacing the photon number operator by its average in the iteration process. Explicitly this is implemented by starting from some initial guess $J_0^{(0)}$, $E_0^{(0)}$, $J^{(0)}$, $E^{(0)}$ in the Hamiltonian (37), from which we calculate the ground state $|\psi^{(0)}\rangle$. By use of this state we obtain an initial mean photon number $\langle\psi^{(0)}|a^\dagger a|\psi^{(0)}\rangle$, with the steady-state field operator (30). Now we can calculate the matrix elements $J_0^{(1)}$, $E_0^{(1)}$, $J^{(1)}$, $E^{(1)}$ again leading to a new ground state $|\psi^{(1)}\rangle$ and a new mean photon number $\langle\psi^{(1)}|a^\dagger a|\psi^{(1)}\rangle$. Proceeding iteratively, in most cases the fixpoint is reached already after very few iterations and the system properties are then calculated with this self-consistent matrix elements. The convergence speed decreases near the resonance for the cavity photon number (cf. Fig. 3), which occurs for $\Delta_c = U_0 J_0 N - \kappa$, especially for large U_0. Introducing some damping in the iteration procedure easily resolves this issue, though. As we mentioned already before, we restrict the model on a subspace $\mathcal{H}_N$ of a fixed total particle number N in an optical lattice of M sites. A basis of $\mathcal{H}_N$ consists of the states $|N,0,0,\ldots,0\rangle, |N-1,1,0,\ldots,0\rangle,\ldots,|0,0,\ldots,0,N\rangle$. Since we are interested in the quantum phase transition between the Mott insulator (MI) and the superfluid (SF) state occurring during the variation of certain external parameters, we investigate the contributions of these specific states to the ground state of the atomic system. The Mott insulator state is a product of Fock states with uniform density distribution, i.e.,

$$|\mathrm{MI}\rangle = |n,n,\ldots,n\rangle, \tag{49}$$

with $n = N/M$. In contrast, in a SF state each atom is delocalized over all sites. It is given by a superposition of Fock states, namely of all possible distributions of the atoms in the lattice sites, i.e.,

$$|\mathrm{SF}\rangle = \sum_{k_1,k_2,\ldots,k_M} \frac{N!}{\sqrt{M^N}\sqrt{k_1!k_2!\cdots k_M!}}|k_1,k_2,\ldots,k_M\rangle, \tag{50}$$

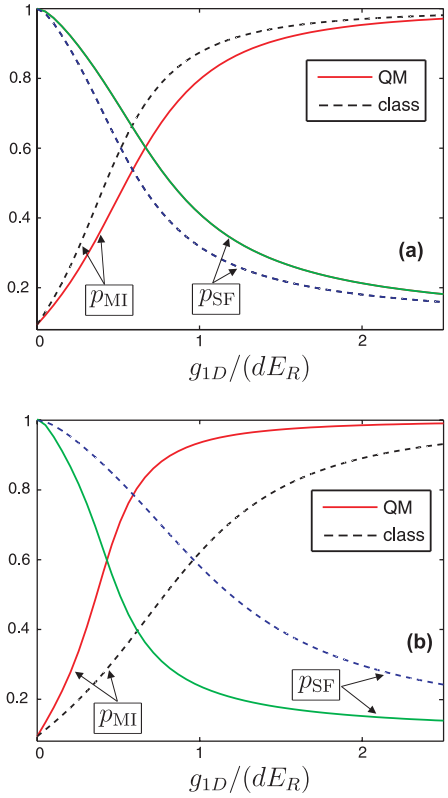

Fig. 4. (Color online) Cavity influence of the Mott insulator to superfluid transition by means of a comparison of the occupation probabilities p_{MI} and p_{SF} for a purely quantum field, i.e., $V_{cl} = 0$, and a purely classical field, i.e., $\eta = 0$, as a function of the dimensionless one-dimensional on-site interaction strength $g_{1D}/(dE_R)$. We choose η such that both potentials are of equivalent depth, $V = 5.5\,E_R$, for zero on-site interaction ($g_{1D} = 0$). The quantum and classical case is depicted with solid and dashed lines, respectively. In (a) we set $(U_0,\kappa,\eta) = (-1, 1/\sqrt{2}, \sqrt{5.5})\,\omega_R$ and $\Delta_c - U_0 J_0 N = \kappa$. (b) The same as (a) but with $\Delta_c - U_0 J_0 N = -\kappa$.

with $\sum_{i=1}^M k_i = N$. Although the density in the superfluid state is also uniform $\langle\hat{n}_i\rangle_{\mathrm{SF}} = N/M$ and therefore equal to the Mott insulator state, its properties are fundamentally different. This manifests especially in the spectra and angle dependence of scattered light, providing for new, non-destructive probing schemes for the atomic phases [34,35].

Let us now investigate the influence of the cavity on position and shape of the well-known "classical" MI-SF-transition [3–5]. To do so, we compare the two cases of a pure quantum field, i.e., $V_{cl} = 0$ in (37), and a classical field ($\eta = 0$) provided by V_{cl} for generating the optical potential. We choose η in such a way, that at zero on-site interaction, $g_{1D} = 0$, both potentials are equally deep. As depicted in Figure 4, the influence of the cavity strongly depends on the detuning Δ_c. Two contributions arise from the quantum nature of the potential. On the one hand the potential depth and therefore the matrix elements depend on the atomic state. For a classical potential this is clearly not the case. On the other hand the cavity mediates long-range interactions via the field, which corresponds to the

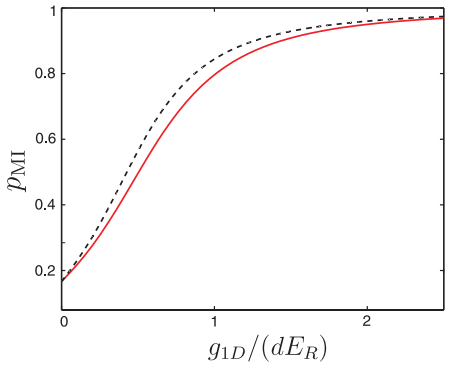

Fig. 5. (Color online) Influence of the long-range interaction on the Mott insulator to superfluid phase transition, mediated via the $\hat{B}^2$ term in (37). The solid line shows the probability for the Mott insulator state as a function of dimensionless one-dimensional on-site interaction strength $g_{1D}/(dE_R)$ for a a purely quantum field, i.e., $V_{cl} = 0$. The dashed line corresponds to the probability for the same Hamiltonian, neglecting the $\hat{B}^2$ term. The parameters are the same as in Figure 4b.

Highlight Paper

$\hat{B}^2$-term in (37). If a potential depth near the phase transition point for the quantum case is associated with some certain average photon number $\bar{n}$, then $\bar{n} \pm 1$ are associated with different atomic phases. This means that the ground state of the quantized cavity field contains contributions of different atomic states, each of them correlated with the corresponding photon number. In this sense photon number fluctuations drive particle fluctuations. Depending on parameters the former or the latter effect contributes more. In Figure 4 this is shown for four atoms in four wells, where we calculated the occupation probability for the Mott insulator $p_{\rm MI} = |\langle\psi|{\rm MI}\rangle|^2$ and the superfluid state $p_{\rm MI} = |\langle\psi|{\rm SF}\rangle|^2$ for the ground state $|\psi\rangle$ of (37) as a function of the dimensionless one-dimensional on-site interaction strength $g_{1D}/(dE_R)$ for a purely classical and a purely quantum case. For $\Delta_c - U_0 J_0 N = \kappa$, photon number fluctuations enhance particle fluctuations, shifting the superfluid to Mott insulator transition to higher values of the on-site interaction (Fig. 4a). However, if we choose $\Delta_c - U_0 J_0 N = -\kappa$, the influence of the atomic state on the potential depth exceeds the cavity-mediated long-range interactions, strongly shifting the transition to lower values of g_{1D} (Fig. 4b). Note, that for this behavior, the cavity loss rate must be – although within the bad cavity limit – small enough. For larger κ the quantum effects disappear and the ground states for classical and quantum potential coincide.

To correctly address the long-range interactions, corresponding to the $\hat{B}^2$ term in (37), we calculate the contribution of the Mott insulator state to the ground state of this adiabatic Hamiltonian including and omitting the $\hat{B}^2$ part, respectively. Although, in the situation of Figure 4b the net effect enhances the phase transition, the cavity mediates long-range coherence via $\hat{B}^2$, which can be seen by enlarged particle number fluctuations as shown in Figure 5. Although the effect is not too strong as it depends on J^2 is has infinite range and will get more important for large particle numbers.

Finally, we exhibit the transition from a cavity field with quantum properties towards a classical optical lattice. This relies on the assumption that a very bad cavity should be almost like no cavity and increasing κ, but keeping the potential depth constant, approaches the classical limit. Hence, the effects of the quantum nature and feedback of lattice potential should disappear and the ground states for classical and quantum potential coincide. The adiabatic eliminated Hamiltonian then has to approach the classical Bose-Hubbard Hamiltonian. This is shown in Figure 6 for a system of four atoms in four wells, where we simultaneously increase κ and η, keeping $U_0\eta^2/\kappa^2 = -6E_R$ fixed. For every κ we calculated the value of the on-site interaction $g_{1\rm D}$, where the contributions of the Mott state and the superfluid state to the ground state of (37) are equal, i.e., $|\langle\psi|{\rm MI}\rangle| = |\langle\psi|{\rm SF}\rangle|$. This is compared with the corresponding value of the interaction strength at the same intersection point of a purely classical Bose-Hubbard model with a potential depth of $V_{cl} = -6E_R$. We see that the transition occurs already at a cavity linewidth of only an order of magnitude larger than the recoil frequency, where the deviation is small already. Thus one needs quite good resonators to see the quantum shift in the phase transition.

3.4 Comparison with the full dynamics of the master equation

Using the approximate adiabatic model with eliminated field we have found important changes in the physics so far. Even stronger effects are to be expected in the limit of less and less cavity damping and stronger atom field coupling. Let us now investigate some first signs of this and test the range of validity of the above model in this limit. To do so we have to resort to numerics and compare solutions of the full master equation (19) with the ground states of the adiabatically eliminated Hamiltonian (37). Obviously solving the full master equation is a numerically demanding task. Nevertheless, by constraining to few atoms in few wells we are able to solve the equations and reveal the essential physical mechanisms. The limit of the band model description is of course reached for atoms coupled strongly to a cavity field with only very few photons and no additional classical potential V_{cl} present. Here very strong changes in the tunneling amplitudes occur whenever a photon leaks out of the cavity and reduces the momentary potential depth. This leads to strongly enhanced particle hopping. For instance, one can think of the situations "one photon present" and "no photon present", where the atoms can freely move within the cavity in the absence of an external trap. On the other hand one extra photon can almost block hopping. Note that in this case the ground state atomic configuration can be close to superfluid for a low photon number and close to an insulator state for a higher photon number. As our matrix elements depend only on the mean photon number

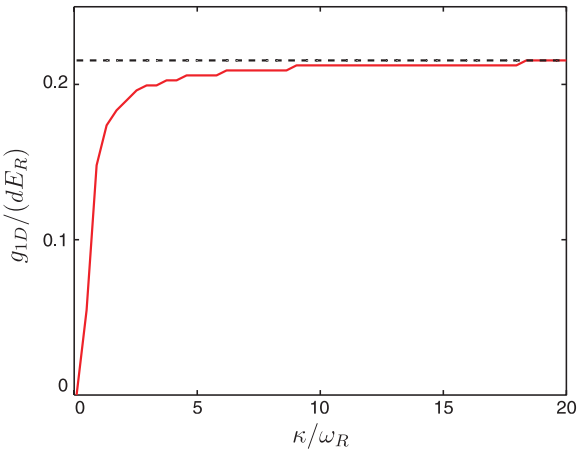

Fig. 6. (Color online) Value of the on-site interaction g_{1D}, where the contributions of the Mott state and the superfluid state to the ground state of (37) are equal, i.e., $|\langle\psi|\mathrm{MI}\rangle| = |\langle\psi|\mathrm{SF}\rangle|$, as a function of κ (solid line) for a system of four atoms in four wells. Simultaneously we increase η, such that $U_0\eta^2/\kappa^2 = -6E_R$ is fixed. Obviously, the corresponding value at the same intersection point of a purely classical Bose-Hubbard Hamiltonian with $V_{cl} = -6E_R$ is constant (dashed line). Parameters are $U_0 = -\omega_R$, $\kappa = 4\omega_R$ and $\Delta_C - U_0 N = -\kappa$.

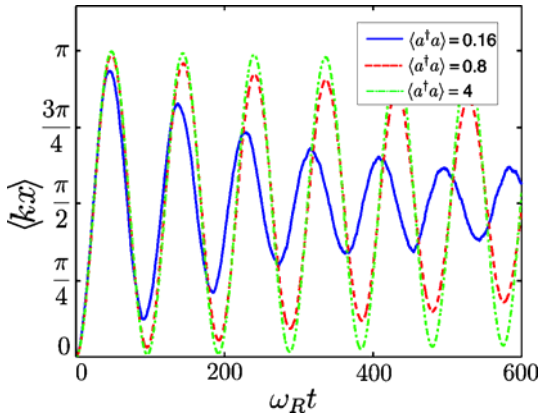

Fig. 7. (Color online) Mean position $\langle kx(t)\rangle$ of a single atom in two wells. We adjusted U_0, η, Δ_c in such a way, that the mean number of cavity photons increases, but the lattice depth stays nearly constant: $V = \hbar U_0\langle a^\dagger a\rangle = -8E_R$. Starting with $(U_0, \eta, \kappa) = (-50, 10, 25)$ (in units of ω_R) and $\Delta_c = J_0 U_0$, followed by a successive reduction of U_0 by a factor of 5, together with an increase of η by a factor of $\sqrt{5}$ and a proper adjustment of Δ_c, this leads to mean photon numbers of 0.16 (solid line), 0.8 (dashed line), and 4 (dashed-dotted line). Initially, the atom is in the right well.

$\langle a^\dagger a\rangle$, these differences cannot be taken into account in an adiabatic model.

We can explicitly show this behavior by reducing the coupling strength U_0, but keeping the average potential depth fixed (equal matrix elements), by means of a higher average cavity photon number, which leads to strongly reduced photon number fluctuations. The most simple situation to discuss this issue is one atom loaded in a lattice consisting of only two wells. Here, $|l\rangle$ ($|r\rangle$) means the left (right) of the two wells, with a potential minimum at $x = 0\,(x = \pi)$. The hopping operator $\hat{B}$ then describes tunneling from the left well to the right well and vice versa. In Figure 7 we show this tunneling behavior by plotting the mean position of the single atom $\langle kx(t)\rangle$. The atomic ground state of this system is the symmetric state $|\psi_0\rangle = (|l\rangle + |r\rangle)/\sqrt{2}$ having a mean position of $\langle kx\rangle_{\psi_0} = \pi/2$. Decreasing U_0, increasing η and adjusting Δ_c, yields different mean photon numbers $\langle a^\dagger a\rangle$, but equal average lattice potential depth $V = U_0\langle a^\dagger a\rangle$. (We do not consider an additional classical potential here.) If only few photons are present, we observe large fluctuations of the field and the system damps fast to the ground state. As the photon number increases, the potential approximates a classical potential as expected, where there is no dephasing. The (nearly) equal oscillation frequencies show that the matrix elements coincide for the different photon numbers. This is an interesting feature corresponding to the quantum nature of the potential. In contrast to the Bose-Hubbard model for a classical optical lattice, lattice depth and interaction strength are not the only important system parameters. Quantum fluctuations of the potential are an additional source of atomic fluctuations, playing an essential role in the evolution of the system. Obviously, if only an external potential is present and the atom is no longer coupled to the cavity field ($U_0 = 0$), the system is undamped, due to the lack of the only dissipation channel present, cavity loss. In this case the Hamiltonian (28) reduces to $H = (E + JV_{cl})\hat{B} + U/2\hat{C}$, and the atom, initially not in the symmetric state, oscillates between the left and right well. Note that a more rigorous treatment of operator-valued matrix elements – as described in the previous section – would be capable of describing this behavior correctly. Alternatively for few atoms Monte Carlo wave function simulations of the full Hamiltonian could be performed, allowing for processes, where the particle leaves the lowest band [54].

Obviously, this enhancement of atom fluctuations for low photon numbers also affects the dynamics of several atoms. We demonstrate this for the case of two atoms in two wells. We assume strong coupling with few cavity photons and a strong on-site interaction, which – in principle – inhibits tunneling and drives the system deeply into the Mott insulator regime. However, starting from a state slightly perturbed from the ground state of the adiabatically eliminated Hamiltonian (37), the system does not evolve towards this Mott-like ground state but towards some other, drastically different state. Increasing the photon number, while keeping the lattice depth constant, reduces the atom fluctuations and keeps the system near its adiabatic ground state. This is shown in Figure 8a, where the probability for the system being in the Mott insulator regime $p_{\mathrm{MI}} = |\psi_{\mathrm{MI}}(t)|^2$ is plotted. Again we observe that, the larger the intracavity photon number is, the more the potential approaches a purely classical one and the more significant the ground state probabilities of (37) are. Hence we see that including the photon

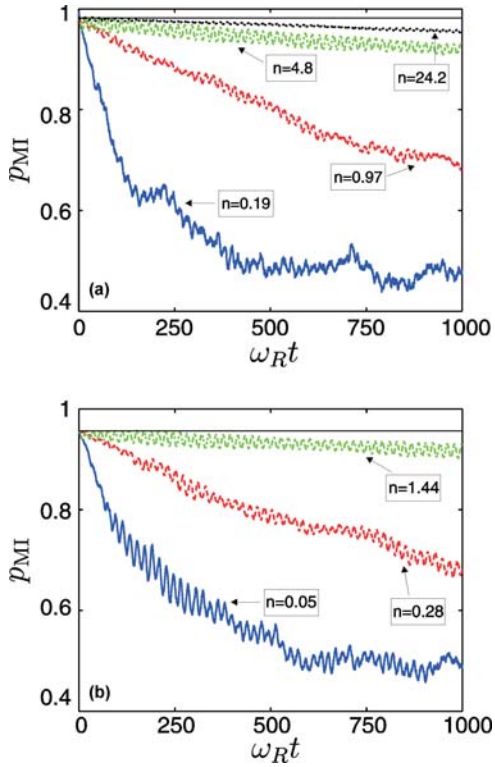

Fig. 8. (Color online) Probability of the Mott insulator state $|\psi_{\rm MI}(t)|^2$ for two atoms in two wells. Parameters and procedure as in Figure 7, but due the second atom the photon numbers are increased. The on-site interaction is $U = 0.32E_R$. (a) $V_{cl} = 0$. The curves correspond to a mean photon number of 0.19 (solid line), 0.97 (dashed line), 4.8 (dashed-dotted line) and 24.2 (dotted line). (b) $V_{cl} = -5E_R$ and corresponding photon numbers of 0.05 (solid line), 0.28 (dashed line), 1.44 (dashed-dotted line).

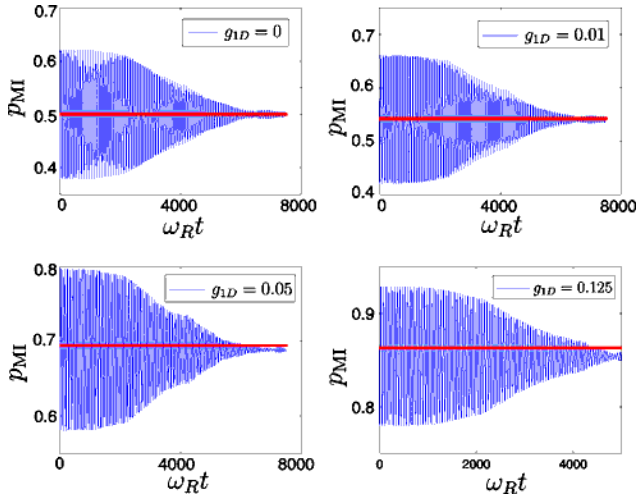

Fig. 9. (Color online) Probability of the Mott insulator state $|\psi_{\rm MI}(t)|^2$ for two atoms in two wells for different on-site interaction. In (a) there is no interaction, i.e., $U = 0$, in (b) $U = 0.0065E_R$, in (c) $U = 0.0324E_R$ and in (d) $U = 0.081E_R$. Other parameters are $(U_0, \kappa, \eta, \Delta_c) = (-50, 25, 1, 0)$ (in units of ω_R), the classical potential is $V_{cl} = -10E_R$. The solid line in each subplot shows the corresponding ground state probability of (37) and the number of cavity photons is $\langle a^\dagger a\rangle = 1.3\times10^{-4}$.

number fluctuations strongly suppresses the Mott insulator state by allowing the particles to hop during photon number fluctuations. This is also a strong restriction for the use of our adiabatic model Hamiltonian, where only average photon numbers enter the model parameters.

Clearly, some added external classical potential diminishes this problem as it can ensure the existence of a bound state, independent of the number of cavity photons, giving an upper limit to the hopping rate. This is demonstrated in Figure 8b, where a classical potential of $V_{cl} = -5E_R$ is added. Here for $\langle a^\dagger a\rangle = 1.44$ the deviations from the adiabatic ground state are of the same order as for $V_{cl} = 0$ for $\langle a^\dagger a\rangle = 4.8$ (Fig. 8a). Nevertheless, for not too leaky cavities (κ is in an intermediate regime), the regime of validity of the adiabatically eliminated Hamiltonian (37) is limited to case where either a large purely classical potential or a large photon number is given.

Finally, we investigate the other limit of validity, where a rather large external classical potential, but only a very low photon number is given, i.e., a weakly driven cavity. Here the ground state properties of our model resemble to a very high degree those of the ordinary Bose-Hubbard model. As mentioned above, an atomic ensemble interacting with a purely classical potential, has no channels of dissipation in the absence of spontaneous emission. So unless we prepare the system in its groundstate, it will show undamped oscillation. In strong contrast the coupling of the atoms to an even small intracavity field with a very low photon number opens a dissipation channel. Although the enhancement of atom number fluctuations due to fluctuation induced tunneling is small, this damping still can drive the system into a steady state, very closely to the adiabatic ground state of (37). This is shown in Figure 9 for the case of two atoms in two wells. Here we prepare, for different values of on-site interaction, the atoms in a state perturbed from the ground state of (37) with initially no photon in the cavity and a given value of the classical potential $V_{cl} = -10E_R$. For $g_{1D} = 0$, the ground state is the superfluid state, so Figure 9a is the generalization of Figure 7 to two atoms. Although the photon number is only $\langle a^\dagger a\rangle = 1.3 \times 10^{-4}$, the system is driven into its ground state. For increasing interaction strength, the Mott insulator state becomes more and more favored. Still, the interaction with the tiny intracavity field enables damping of the atomic evolution towards a steady state, very close to the adiabatic ground state.

This leads to the conclusion, that, although the cavity field may not lead to significant modifications of the ground state of the system, the cavity is a useful tool for faster preparing a system of atoms in its ground state by opening a dissipation channel, so that it decays towards an eigenstate of the adiabatically eliminated Hamiltonian (37).

4 Atom pumping

Let us now return to our starting Hamiltonian (26) and consider a second generic model, where the pump laser is not injected through the cavity mirrors, but directly

illuminating the atoms. This rather small change has a drastic influence on the physical behavior of this system. In the case of cavity pumping, all atoms are simultaneously coupled to the same mode. In this way the cavity field depends on the atomic distribution and long range order interactions are mediated via the cavity field, influencing the Mott-insulator to superfluid phase transition. In the new geometry, only the directly excited atoms coherently scatter photons in the cavity mode. Due to the position-dependent coupling, the scattered field amplitude and phase for each atom is strongly position dependent. Atoms located at nodes are not coupled to the field, leading to no scattering, whereas atoms at antinodes are maximally coupled, leading to maximum scattering. Atoms in adjacent wells are separated by half a wavelength and scatter with opposite phases, such that their contributions to the scattered field interferes destructively. Naively one would thus immediately conclude that atoms forming a state with a homogeneous density scatter no field at all so that nothing happens [34,35]. Nevertheless, fluctuations of the density still can allow for some background scattering which should diminish for lower temperature. For suitable parameters the corresponding forces start to reorder the atoms towards a periodic pattern of the atoms, where scattering is strongly enhanced. This then deepens the optical potential, stabilizing the pattern in a self-organizing runaway process, semiclassically described in [18].

At $T = 0$ quantum fluctuations still can trigger this reorganization. To study this effect we assume the coherent pump field to form a broad plane wave propagating transversally to the cavity axis (see Fig. 1) replacing cavity pumping. This means that we set $\eta = 0$ and the Hamiltonian (26) for constant atom number N reads as follows:

$$H = (E + JV_{\rm cl})\,\hat{B} + \hbar\,(U_0 J_0 N - \Delta_c)\,a^\dagger a + \frac{U}{2}\hat{C} + \hbar U_0 J a^\dagger a \hat{B} + \hbar\eta_{\rm eff}\left(a + a^\dagger\right)\tilde{J}_0\hat{D}. \quad (51)$$

Here we introduced the operator $\hat{D} = \sum_k (-1)^{k+1}\hat{n}_k$ describing the difference in atom number between odd and even sites. The corresponding Heisenberg equation for the cavity field (27) reads as follows:

$$\dot{a} = \left\{ i\left[\Delta_c - U_0\left(J_0 N + J\hat{B}\right)\right] - \kappa\right\} a - i\eta_{\rm eff}\tilde{J}_0\hat{D}. \quad (52)$$

Consequently the Heisenberg equation for the particle operators is:

$$\dot{b}_k = \left(E + JV_{cl} - iU_0 J a^\dagger a\right)\left(b_{k+1} + b_{k-1}\right) - i\eta_{\rm eff}\tilde{J}_0\left(a + a^\dagger\right)(-1)^{k+1} b_k + U\hat{n}_k b_k. \quad (53)$$

Hence we see that the occupation number difference drives the cavity field, which then in turn starts to dephase neighboring atom sites via the first term in the second line of equation (53). Note that this interesting part of the dynamics even survives for deeper lattices when J is negligibly small and $\tilde{J}_0$ is of order unity. This will discussed in more detail using various approximations below.

4.1 Field-eliminated Hamiltonian

Adiabatic elimination of the field variables is a bit more subtle here as compared to the cavity pump case discussed before. The scattering amplitude of light into the cavity mode here depends strongly on the atomic positions. Hence even small position changes have a large influence on the cavity field dynamics. The maximum photon number is established when all the atoms are well localized at either only odd or only even lattice sites. For red atom field detuning this increases the lattice depth and forces the atoms into one of two stable patterns, where the wells where atoms are located are deeper than the empty ones. Hence this changes the translational periodicity of the optical lattice from $\lambda/2$ to λ. Such bistable behavior was observed by Vuletić and coworkers [20] and explained in a semiclassical treatment [18].

Let us now turn to a quantum treatment of atoms and field. Naive adiabatic elimination encounters a first difficulty, as the operators $\hat{B}, \hat{D}$ do not commute, $[\hat{B}, \hat{D}] \neq 0$. Hence this already creates an ordering problem in the formal steady-state solution of (52), which gets even more difficult when it comes to the replacement of the field operators to obtain an effective Hamiltonian (51). Unfortunately also the second approach used in the case of cavity pumping, namely reading off an effective Hamiltonian from the particle operator Heisenberg equation does not resolve this problems. Replacing a with the steady-state expression in (53) leads to a rather complex form, so that there is no simple way to find a suitable effective Hamiltonian $H_{\rm ad}$, with $i\hbar\dot{b}_k = [b_k, H_{\rm ad}]$.

Hence we have to resort to the further approximation of neglecting the term $\hbar U_0 J a^\dagger a\hat{B}$, compared to JV_{cl}. This still leaves the most important part of the new physics, but reduces the field equation to the form:

$$\dot{a} = (i\Delta_c' - \kappa)\,a - i\eta_{\rm eff}\tilde{J}_0\hat{D}. \quad (54)$$

The steady-state solution of this equation is immediately at hand and free of ordering ambiguities of noncommuting operators.

$$a = \frac{i\eta_{\rm eff}\tilde{J}_0}{i\Delta_c' - \kappa}\hat{D}. \quad (55)$$

Also the particle operator equation is much simpler within this approximation:

$$\dot{b}_k = (E + JV_{cl})\left(b_{k-1} + b_{k+1}\right) - i\eta_{\rm eff}\tilde{J}_0\left(a + a^\dagger\right)(-1)^{k+1} b_k + U\hat{n}_k b_k. \quad (56)$$

In this form one then can find a well defined effective Hamiltonian only containing particle operators. Let us thus proceed as in Section 3.1 and simply substitute (55) and its adjoint into (51). This yields the effective Hamiltonian:

$$H_{\rm ad} = (E + JV_{\rm cl})\hat{B} + \frac{U}{2} + \frac{\hbar\tilde{J}_0^2\eta_{\rm eff}^2\Delta_c'}{\kappa^2 + {\Delta_c'}^2}\hat{D}^2. \quad (57)$$

Within first order in J the replacement of the field variables in the Liouvillean part of the master equation (20) in this case does not provide an extra terms to be included in the Hamiltonian. So the effective cavity decay induced dissipation of the atomic dynamics takes the simple and intuitive form:

$$\mathcal{L}_{\rm ad}\,\varrho = \frac{\kappa\eta_{\rm eff}^2\tilde{J}_0^2}{\kappa^2+{\Delta_c'}^2}\left(2\hat{D}\varrho\hat{D}-\hat{D}^2\varrho-\varrho\hat{D}^2\right). \tag{58}$$

Note that equation (57) with the replacement of the field operator by its steady-state expression also leads to the same time evolution as induced by (56) after symmetrizing with respect to the field terms. The two approaches thus lead to identical predictions, which we will exhibit in some more detail in the following.

4.2 Self-organization of atoms in an optical lattice

In this section we investigate the microscopic dynamics of self-ordering near zero temperature and compare the results of the general model Hamiltonian (51) and the corresponding effective Hamiltonian (57). In order to simplify things, we keep the approximation from above and neglect $JU_0a^\dagger a$ in the model, i.e.,

$$H = (E+JV_{\rm cl})\,\hat{B} - \hbar\Delta_c' a^\dagger a + \frac{U}{2}\hat{C} + \hbar\eta_{\rm eff}\tilde{J}_0\hat{D}\left(a+a^\dagger\right), \tag{59}$$

with $\Delta_c' = \Delta_c - U_0J_0N$. Let us point out here, that the Hamiltonian in this approximative form is equivalent to a Hamiltonian describing 1D motion along an optical lattice transverse to the cavity axis. Such a lattice can e.g. be generated by the pump laser itself as it was studied in [55,56] to investigate the onset of the self-organization process [18–20] at zero temperature.

Similar to that case, the effective Hamiltonian equation (59) for moderate coupling reproduces quite well the results of a full Monte Carlo wavefunction simulation. We have checked this for a rather small system of two atoms in two wells with periodic boundary conditions. This is the minimal system to study self-organization but in general sufficient to capture the physics. In this special case the operator $\hat{B}$ simply couples the ordered $|11\rangle$ state to the state $1/\sqrt{2}\,(|20\rangle+|02\rangle)$, while the operator $\hat{D}^2$ leaves all the basis states $\{|11\rangle,|20\rangle,|02\rangle\}$ unchanged. It simply leads to a relative energy shift. Hence starting from a perfectly ordered atomic state (the analog of the Mott insulator state) the Hamiltonian part of the time evolution of the system couples it to the symmetric superposition of ordered states. In an adiabatic limit those ordered states are correlated with a coherent field $\pm\alpha$ in the cavity. Thus without damping the evolution would simply read:

$$|\psi(t)\rangle = \cos(2\omega t)\,|1,1,0\rangle + \frac{i\sin(2\omega t)}{\sqrt{2}}\,(|20,2\alpha\rangle+|02,-2\alpha\rangle). \tag{60}$$

where the frequency ω is given by the $(E+JV_{\rm cl})/\hbar$. Here $|11,0\rangle$ is the state with one atom in each well and zero photons, whereas $|20,\alpha\rangle$ ($|02,-\alpha\rangle$) corresponds to the state with both atoms in the left (right) well, and the cavity field being in a coherent state with amplitude 2α (-2α). The factor 2 is due to constructive interference of the fields, scattered by the ordered atoms. In the Mott state, the scattering fields cancel each other.

Note that such an entangled superposition of different atomic states and fields cannot be reproduced by any classical or mean field evolution and requires a genuine quantum description. If on-site interaction is added the amplitude of this oscillations decreases due to extra relative different phase changes of the self-ordered and the Mott state.

Of course we now have to add the effect of dissipation via cavity loss. We will see that even single cavity photon decay events strongly perturb the system evolution. This can be immediately seen by applying the photon annihilation operator to the entangled atom-field state, i.e.,

$$|\psi(t)'\rangle \propto a|\psi(t)\rangle \propto |20,2\alpha\rangle - |02,-2\alpha\rangle. \tag{61}$$

This procedure projects out the Mott contributions to the state as they are connected to zero photons. Surprisingly in addition it also blocks further tunneling by introducing a minus sign between the two ordered states. At this point coherent atomic time evolution stops until a second photon escapes and re-establishes the plus sign. This then allows tunnel coupling back to the Mott insulator state again. In this sense self-ordering is an instantaneous projective process here, where the cavity acts as measurement apparatus asking a sort of yes/no ordering question.

The fact, that for transverse pumping the adiabatic field state associated with the Mott insulator is an intracavity vacuum decouples this state from further dynamics even in the presence of dissipation. This creates numerical difficulties and prohibits an approximation of the dissipative dynamics by the adiabatic ground state values of (57) only. As soon as a photon leaks out of the cavity, the contribution of the Mott-insulator state is canceled, no matter how large it, corresponding to a given on-site interaction, might be. Hence, every initial state evolves into a superposition of the ordered states and the ground state values of the effective Hamiltonian do not make much sense. Nevertheless, including the damping via the effective Liouvillean (58) approximately reveals the complete dynamics. In Figure 10 we show the results of a Monte Carlo simulation of the dynamics of the Mott and the superfluid contribution, corresponding to (59) and compare it with a solution of the master equation, consisting of the Hamiltonian (57) and Liouvillean (58), where the field variables are eliminated. Furthermore, the restriction of the Hilbert space to the two states of (61) and $|11,0\rangle$, allows for a proof of the accuracy of our assumption, concerning the fast evolution of the cavity field. We use the coefficients $c(t),\tilde{c}(t)$ (calculated with the Monte Carlo simulation) of $|\psi(t)\rangle = \tilde{c}(t)|11,0\rangle + c(t)(|20,2\alpha\rangle \pm |02,-2\alpha\rangle)$ to construct a purely atomic state $|\varphi(t)\rangle = \tilde{c}(t)|11\rangle + c(t)(|20\rangle \pm |02\rangle)$. Then the

Highlight Paper

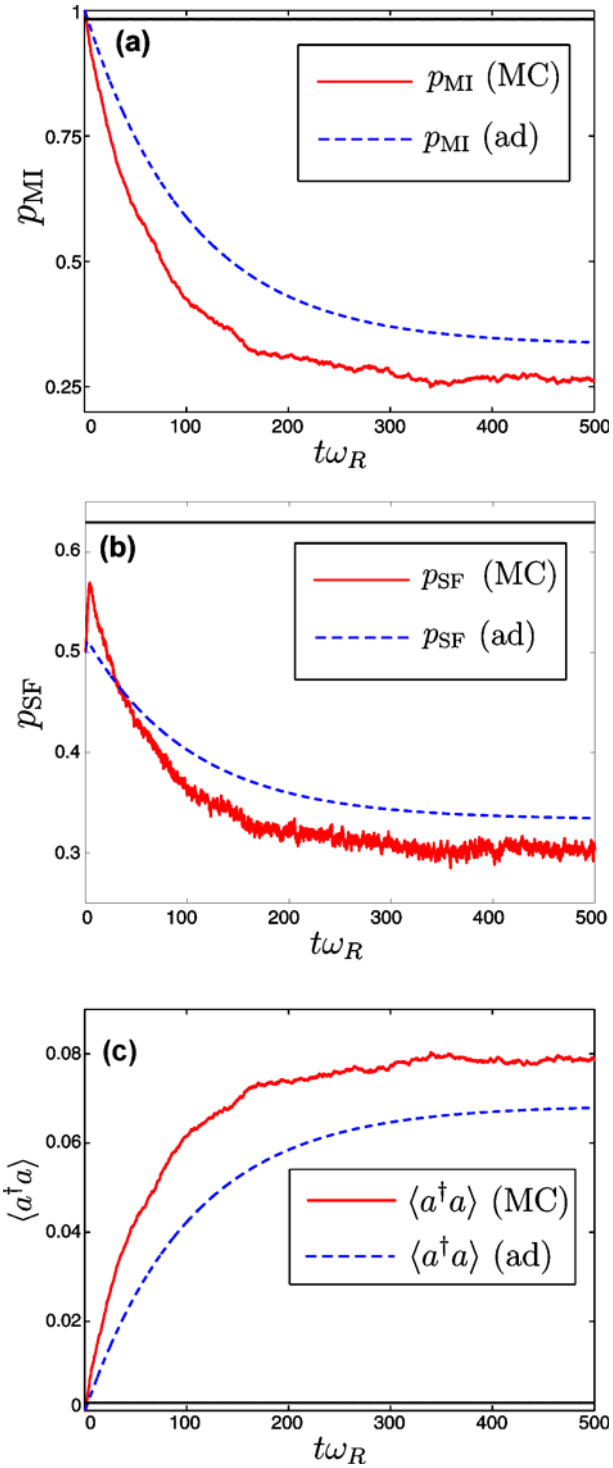

Fig. 10. (Color online) (a) Contribution of the Mott insulator state $p_{\rm MI}$ in a system of two atoms in two wells. The solid line shows the results of a Monte Carlo simulation, corresponding to (59) with dissipation via cavity loss. The dashed line depicts the solution of a master equation with effective Hamiltonian (57) and Liouvillean (58). The constant line, shows the ground state value of this contribution of the effective Hamiltonian. (b) The same for the contribution of the superfluid state $p_{\rm SF}$. (c) Shows analogue results for the mean photon number. Parameters are $V_{\rm cl} = -10E_R$, $(\kappa, U_0, \eta_{\rm eff}) = (4, -0.1, 1)\,\omega_R$ and $\Delta_c = U_0 J_0 N + \kappa$.

mean photon number, calculated with the effective photon operator (55) agrees very well with the real mean photon number, i.e.,

$$\frac{\eta_{\rm eff}^2 \tilde{J}_0^2}{{\Delta_c'}^2 + \kappa^2}\langle\varphi(t)|\hat{D}^2|\varphi(t)\rangle \approx \langle\psi(t)|a^\dagger a|\psi(t)\rangle. \qquad (62)$$

5 Conclusions

Based on an approximative Bose-Hubbard type model descriptions, we have shown that quantum characteristics of light fields generating optical potentials lead to shifts in quantum phase transition points and play a decisive role in the microscopic dynamics of the transition process. While many physical aspects can be already captured by effective Hamiltonians with rescaled parameters, cavity mediated long-range interactions also play an important role and add a new nonlocal element to optical lattices dynamics for atoms. In that context even small modifications in the setup, from cavity pump to transverse pump, have a drastic influence on the behavior of the system on a microscopic level. We have seen that the Bose-Hubbard Hamiltonian for the former system can, in a certain parameter regime, be significantly simplified by adiabatically eliminating the field variables. Although the cavity has influence on its shape, the Mott insulator to superfluid phase transition occurs similar to classical optical lattices. For transverse pumping this is not the case. Here, the fields scattered by the atoms in the uniform Mott state cancel and completely suppress scattering. In parallel new ordered states with maximal coupling of pump and cavity field appear and the dynamics favors a superposition of these two ordered states correlated with coherent field states with phase difference π. Hence the dynamics generates strong atom field entanglement and large effective optical nonlinearities even in the limit of linear weak field scattering.

Of course the various approximations used to derive our effective Hamiltonians still leave a lot of room for improvements and we could only touch a very small part of the physical effects and possibilities contained in these model. Fortunately the experimental progress in this field is spectacularly fast and several groups now have set up optical lattices with cavity fields [36–40] and intriguing potential applications of such systems were already proposed [57], so that one can expect a fast and exciting further development of this field.

The authors would like to thank M. Lewenstein, G. Morigi, S. Fernández-Vidal, A. Micheli, and A. Vukics for useful discussions. This work was funded by the Austrian Science Fund (P17709 and S1512). After completion of this work we became aware of related parallel work by M. Lewenstein and coworkers, which treats many aspects of this model in the thermodynamic limit [58].

References

1. See e.g. *Laser Manipulation of Atoms and Ions*, edited by E. Arimondo, W.D. Phillips, Varenna Summer School, 1991 (North-Holland, Amsterdam, 1992)
2. I. Bloch, Nature Phys. **1**, 23 (2005); I. Bloch, M. Greiner, Adv. At. Mol. Opt. Phys. **52**, 1 (2005)
3. D. Jaksch, C. Bruder, J.I. Cirac, C.W. Gardiner, P. Zoller, Phys. Rev. Lett. **81**, 3108 (1998)
4. W. Zwerger, J. Opt. B **5**, 9 (2003)
5. M.P.A. Fisher, P.B. Weichman, G. Grinstein, D.S. Fisher, Phys. Rev. B **40**, 546 (1989)
6. M. Greiner, O. Mandel, T. Esslinger, T.W. Hänsch, I. Bloch, Nature **415**, 39 (2002); M. Greiner, O. Mandel, T.W. Hänsch, I. Bloch, Nature **419**, 51 (2002)
7. D. Jaksch, P. Zoller, Ann. Phys. **315**, 52 (2005)
8. S. Inouye, M.R. Andrews, J. Stenger, H.-J. Miesner, D.M. Stamper-Kurn, W. Ketterle, Nature **392**, 151 (1998)
9. M. Theis, G. Thalhammer, K. Winkler, M. Hellwig, G. Ruff, R. Grimm, J. Hecker Denschlag, Phys. Rev. Lett. **93**, 123001 (2004)
10. T. Stöferle, H. Moritz, C. Schori, M. Köhl, T. Esslinger, Phys. Rev. Lett. **92**, 130403 (2004)
11. M. Köhl, H. Moritz, T. Stöferle, C. Schori, T. Esslinger, J. Low Temp. Phys. **138**, 635 (2005)
12. I.B. Spielman, W.D. Phillips, J.V. Porto, Phys. Rev. Lett. **98**, 080404 (2007)
13. B. Paredes, A. Widera, V. Murg, O. Mandel, S. Fölling, I. Cirac, G.V. Shlyapnikov, T.W. Hänsch, I. Bloch, Nature **429**, 277 (2004)
14. T. Kinoshita, T.R. Wenger, D.S. Weiss, Science **305**, 1125 (2004)
15. Z. Hadzibabic, P. Krüger, M. Cheneau, B. Battelier, J. Dalibard, Nature **441**, 1118 (2006)
16. M. Lewenstein, A. Sanpera, V. Ahufinger, B. Damski, A. Sen De, U. Sen, Adv. Phys. **56**, 243 (2007)
17. P. Domokos, H. Ritsch, J. Opt. Soc. Am. B **20**, 1098 (2003)
18. P. Domokos, H. Ritsch, Phys. Rev. Lett. **89**, 253003 (2002)
19. S. Zippilli, G. Morigi, H. Ritsch, Phys. Rev. Lett. **93**, 123002 (2004)
20. A.T. Black, H.W. Chan, V. Vuletić, Phys. Rev. Lett. **91**, 203001 (2003)
21. P.W.H. Pinkse, T. Fischer, P. Maunz, G. Rempe, Nature **404**, 365 (2000)
22. C.J. Hood, T.W. Lynn, A.C. Doherty, A.S. Parkins, H.J. Kimble, Science **287**, 1447 (2000)
23. P. Horak, G. Hechenblaikner, K.M. Gheri, H. Stecher, H. Ritsch, Phys. Rev. Lett. **79**, 4974 (1997); G. Hechenblaikner, M. Gangl, P. Horak, H. Ritsch, Phys. Rev. A **58**, 3030 (1998)
24. V. Vuletić, H.W. Chan, A.T. Black, Phys. Rev. A **64**, 033405
25. P. Domokos, A. Vukics, H. Ritsch, Phys. Rev. Lett. **92**, 103601 (2004)
26. S. Zippilli, G. Morigi, H. Ritsch, Phys. Rev. Lett. **95**, 143001 (2005)
27. P. Maunz, T. Puppe, I. Schuster, N. Syassen, P.W.H. Pinkse, G. Rempe, Nature **428**, 50 (2004)
28. S. Nußmann, K. Murr, M. Hijlkema, B. Weber, A. Kuhn, G. Rempe, Nature Phys. **1**, 122 (2005)
29. A. Griessner, D. Jaksch, P. Zoller, J. Phys. B **37**, 1419 (2004)
30. P. Horak, S.M. Barnett, H. Ritsch, Phys. Rev. A **61**, 033609 (2000)
31. D. Jaksch, S.A. Gardiner, K. Schulze, J.I. Cirac, P. Zoller, Phys. Rev. Lett. **86**, 4733 (2001)
32. C. Maschler, H. Ritsch, Phys. Rev. Lett. **95**, 260401 (2005)
33. J. Larsson, B. Damski, G. Morigi, M. Lewenstein, e-print `arXiv:cond-mat/0608335`
34. I.B. Mekhov, C. Maschler, H. Ritsch, Phys. Rev. Lett. **98**, 100402 (2007); I.B. Mekhov, C. Maschler, H. Ritsch, Phys. Rev. A **76**, 053618 (2007)
35. I.B. Mekhov, C. Maschler, H. Ritsch, Nature Phys. **3**, 319 (2007)
36. A. Öttl, S. Ritter, M. Köhl, T. Esslinger, Phys. Rev. Lett. **95**, 090404 (2005); T. Bourdel, T. Donner, S. Ritter, A. Öttl, M. Köhl, T. Esslinger, Phys. Rev. A **73**, 43602 (2006)
37. P. Treutlein, D. Hunger, S. Camerer, T.W. Hänsch, J. Reichel, Phys. Rev. Lett. **99**, 140403 (2007); Y. Colombe, T. Steinmetz, G. Dubois, F. Linke, D. Hunger, J. Reichel, Nature **450**, 272 (2007)
38. F. Brennecke, T. Donner, S. Ritter, T. Bourdel, M. Köhl, T. Esslinger, Nature **450**, 268 (2007)
39. S. Slama, G. Krenz, S. Bux, C. Zimmermann, Ph.W. Courteille, Phys. Rev. A **75**, 063620 (2007)
40. S. Gupta, K.L. Moore, K.W. Murch, D.M. Stamper-Kurn, e-print `arXiv:quant-ph/0706.1052`
41. J. McKeever, J.R. Buck, A.D. Boozer, A. Kuzmich, H.-C. Nägerl, D.M. Stamper-Kurn, H.J. Kimble, Phys. Rev. Lett. **90**, 133602 (2003)
42. T. Puppe, I. Schuster, P. Maunz, K. Murr, P.W.H. Pinkse, G. Rempe, Phys. Rev. Lett. **99**, 013002 (2007)
43. E.T. Jaynes, F.W. Cummings, Proc. IEEE **51**, 89 (1963)
44. See, for example, A. Galindo, P. Pascual, *Quantum Mechanics II* (Springer, Berlin, 1990)
45. K. Huang, *Statistical Mechanics* (John Wiley & Sons, New York, 1987)
46. M. Olshanii, Phys. Rev. Lett. **81**, 938 (1998)
47. C. Maschler, H. Ritsch, Phys. Rev. Lett. **95**, 260401 (2005)
48. C. Kittel, *Quantum Theory of Solids* (John Wiley & Sons, New York, 1963)
49. See, for example, C.W. Gardiner, P. Zoller, *Quantum Noise*, 3rd Edn. (Springer, Berlin, 2005)
50. R. Grimm, M. Weidemüller, Y.B. Ovchinnikov, Adv. At. Mol. Opt. Phys. **42**, 95 (2000)
51. J. Ye, D.W. Vernooy, H.J. Kimble, Phys. Rev. Lett. **83**, 4987 (1999)
52. J.A. Sauer, K.M. Fortier, M.S. Chang, C.D. Hamley, M.S. Chapman, Phys. Rev. A **69**, 051804 (2004)
53. H.M. Wiseman, G.J. Milburn, Phys. Rev. A **47**, 642 (1993)
54. A. Vukics, H. Ritsch, Eur. Phys. J. D **44**, 585 (2007)
55. C. Maschler, H. Ritsch, A. Vukics, P. Domokos, Opt. Commun. **273**, 446 (2007)
56. A. Vukics, C. Maschler, H. Ritsch, New J. Phys. **9**, 255 (2007)
57. D. Meiser, J. Ye, M.J. Holland, e-print `arXiv:quant-ph/0707.3834`
58. J. Larson, S. Fernández-Vidal, G. Morigi, M. Lewenstein, e-print `arXiv:cond-mat/0710.3047`

Highlight Paper